Materials Today Advances 30 (2026) 100853

Contents lists available at ScienceDirect

Materials Today Advances

journal homepage: www.journals.elsevier.com/materials-today-advances/

In vitro cytotoxicity evaluation of green-synthesized nano-hydroxyapatite from eggshell waste using banana extract (*Musa acuminata Cavendish*)

Atiek Rostika Noviyanti [a,b,*], Ferli Septi Irwansyah [c], Alfi Ikhlasul Amal [a], Diana Rakhmawaty Eddy [a], Risdiana Risdiana [d], Yaya Rukayadi [e]

[a] Department of Chemistry, Universitas Padjadjaran, Jl. Raya Bandung-Sumedang KM 21, Jatinangor, Sumedang, 45363, Indonesia
[b] Research Collaboration Center for Microbial Nanomaterials between BRIN and Universitas Padjadjaran, Sumedang 45363, Indonesia
[c] Department of Chemistry Education, UIN Sunan Gunung Djati Bandung, Jl. A.H. Nasution, No. 105, Bandung, 40614, Indonesia
[d] Department of Physics, Universitas Padjadjaran, Jl. Raya Bandung-Sumedang KM 21, Jatinangor, Sumedang, 45363, Indonesia
[e] Department of Food Science, Faculty of Food Science and Technology, Universiti Putra Malaysia, Serdang, Selangor, 43400, Malaysia

ARTICLE INFO

Keywords:
Hydroxyapatite
Eggshell
Cytotoxicity
Nano-HA
Drug delivery
CV-1 cell
Resazurin

ABSTRACT

Hydroxyapatite (HA) is a promising bioceramic material for biomedical applications due to its biocompatibility and bioactivity. In this study, nano-hydroxyapatite (nano-HA) was synthesized from chicken eggshell waste using banana (*Musa acuminata* Cavendish) extracts as green templating agents. Three nano-HA variants derived from banana flower (NHA230B15), pseudostem (NHA230K15), and peel (NHA230P15) were evaluated for in vitro cytotoxicity against normal CV-1 cells using the resazurin reduction assay. NHA230K15 and NHA230P15 maintained cell viability above the ISO 10993-5 cytotoxicity threshold throughout the tested concentration range up to 1000 μg/mL, whereas NHA230B15 showed reduced viability at the highest concentration tested, approaching the cytotoxicity threshold. Morphological observations revealed that treated cells generally retained normal fibroblast-like morphology and membrane integrity without severe structural damage. Differences in cellular response may be associated with variations in the physicochemical characteristics of the synthesized materials. Overall, the banana-template-derived nano-HA materials demonstrated favorable cytocompatibility toward CV-1 cells under the tested in vitro conditions. These findings provide a preliminary assessment of the biological response of green-synthesized nano-HA materials and support further investigation of their potential biomedical relevance. Further studies involving additional cell models, mechanistic evaluation, long-term biocompatibility, and *in vivo* evaluation are still required.

1. Introduction

The application of nanotechnology in biomedical fields has advanced significantly, particularly in the development of biocompatible materials for bone regeneration, tissue engineering, and drug carrier-related systems. Among various bioceramic materials, hydroxyapatite (HA) has attracted considerable attention due to its close resemblance to the mineral phase of human bone and teeth, as well as its excellent biocompatibility, bioactivity, and osteoconductivity [1]. Nano-sized hydroxyapatite (nano-HA) exhibits enhanced surface reactivity and larger surface area compared with bulk HA, which can improve cellular adhesion, proliferation, and biomolecular interactions [2–4]. In addition, hierarchical nanostructured biomaterials have been increasingly explored because their porosity and tunable surface characteristics may support various biomedical functions, including therapeutic agent incorporation and tissue integration. Nevertheless, highly reactive nanostructures may also present limitations, such as particle aggregation, ion release, oxidative stress induction, and potential cytotoxicity, depending on their physicochemical properties and biological exposure conditions [5]. Similar structure-dependent behavior has also been discussed in other nanomaterial systems, where morphology and porosity strongly influence biological and functional performance [6,7].

Among plant-based templates, banana (*Musa acuminata* Cavendish) has demonstrated considerable potential for green synthesis of HA. Different banana plant parts, including flower, pseudostem, and peel, possess distinct fibrous architectures and biopolymeric compositions that may influence hydroxyapatite crystallization, morphology, and surface characteristics. Previous studies reported that banana-derived

* Corresponding author. Department of Chemistry, Universitas Padjadjaran, Jl. Raya Bandung-Sumedang KM 21, Jatinangor, Sumedang, 45363, Indonesia.
E-mail address: atiek.noviyanti@unpad.ac.id (A.R. Noviyanti).

https://doi.org/10.1016/j.mtadv.2026.100853
Received 7 April 2026; Received in revised form 8 June 2026; Accepted 9 June 2026
Available online 11 June 2026

templates can facilitate the formation of porous and biomimetic HA structures with improved physicochemical properties [8,9]. In our previous work, nano-HA synthesized using banana flower, pseudostem, and peel templates exhibited distinct physicochemical characteristics, including differences in crystallite size, crystallinity, particle size, surface area, and morphology [10]. NHA230B15 showed the highest specific surface area, whereas NHA230K15 and NHA230P15 exhibited higher crystallinity and more ordered crystal structures. Such variations are expected to influence nano–bio interactions, particularly cellular responses associated with surface reactivity and particle morphology.

Despite the increasing development of green-synthesized nano-HA materials, most studies primarily focus on synthesis optimization and physicochemical characterization, while systematic biological safety evaluation remains limited. This issue is particularly important because nano-HA particles can interact with biological systems in a size-, morphology-, and surface-dependent manner. Previous studies demonstrated that nano-HA cytotoxicity is strongly influenced by particle size, morphology, aggregation behavior, and surface properties [11]. Certain nano-HA morphologies may induce oxidative stress, mitochondrial dysfunction, and membrane destabilization following cellular internalization [5]. Furthermore, excessive nano-HA exposure has been associated with adverse biological effects, including vascular disruption and oxidative damage in non-target organisms [12,13].These findings highlight the importance of evaluating the cytotoxicity of green-synthesized nano-HA materials, particularly toward normal mammalian cells.

Therefore, this study aimed to investigate the in vitro cytotoxicity of three banana-template-derived nano-HA variants, namely NHA230B15, NHA230K15, and NHA230P15, using normal CV-1 fibroblast cells. It was selected as a representative non-transformed mammalian cell model to provide an initial evaluation of general cytocompatibility. While such cells are suitable for preliminary safety screening, they do not fully represent the biological complexity of bone-regeneration or immune-related applications. Consequently, future investigations involving osteoblasts, mesenchymal stem cells, macrophages, and other clinically relevant cell models will be necessary to establish the broader biomedical applicability of the synthesized nano-HA materials. Cell viability was evaluated using the resazurin reduction assay (PrestoBlue™), which is widely recognized as a reliable method for assessing cellular metabolic activity and mitochondrial integrity [14]; [15]. By correlating differences in template origin and physicochemical characteristics with biological response, this study provides an initial safety-oriented evaluation of green-synthesized nano-HA materials for prospective biomedical and biomaterial-related applications.

2. Methods

2.1. Materials

Nano-hydroxyapatite (nano-HA) samples were synthesized via a hydrothermal method using calcium precursors derived from chicken eggshell waste and banana (*Musa acuminata* Cavendish) plant extracts as natural templating agents. Three distinct nano-HA variants were employed in this study based on the banana plant part used during synthesis, namely banana flower (B), pseudostem (K), and peel (P), denoted as NHA230B15, NHA230K15, and NHA230P15, respectively. The detailed synthesis procedure, calcination conditions, and physicochemical characterization, including phase identification by X-ray diffraction (XRD), crystallite size estimation using the Scherrer equation, Brunauer–Emmett–Teller (BET) surface area analysis, and morphology evaluation using scanning electron microscopy (SEM), have been reported previously [10]. The same material batches were utilized in the present study to ensure experimental consistency and reproducibility.

Cell culture reagents included RPMI-1640 medium (Gibco, USA), fetal bovine serum (FBS, Gibco, USA), penicillin–streptomycin solution (Sigma-Aldrich, USA), trypsin–EDTA (Gibco, USA), phosphate-buffered saline (PBS, Gibco, USA), and trypan blue stain (Sigma-Aldrich, USA). PrestoBlue™ Cell Viability Reagent (Thermo Fisher Scientific, USA) was used for cytotoxicity assessment. Cisplatin (European Directorate for the Quality of Medicines, EDQM) served as a positive cytotoxic control. Dimethyl sulfoxide (DMSO, Merck, Germany) was used as the vehicle control.

2.2. Cell viability assay procedure

CV-1 cells (normal monkey kidney fibroblast cells, *Cercopithecus aethiops*) were cultured in RPMI-1640 medium supplemented with 10% (v/v) FBS and 1% (v/v) penicillin–streptomycin under standard incubation conditions (37 °C, 5% CO_2, and 95% relative humidity). Cells were maintained until reaching approximately 70–80% confluency, then detached using trypsin–EDTA and counted using the trypan blue exclusion method.

Cells were seeded into 96-well plates at a density of approximately 1.7×10^4 cells per well in 100 μL of complete medium and incubated for 24 h to allow cellular attachment. After incubation, the culture medium was replaced with fresh medium containing nano-HA samples at various concentrations up to 1000 μg/mL. Vehicle control (DMSO) and positive control (cisplatin) treatments were included for comparison. Each experimental condition was performed in triplicate ($n = 3$), and all data are presented as mean ± standard deviation.

Following 24 h of exposure, the treatment medium was removed and replaced with 100 μL of PrestoBlue™ working solution prepared by diluting the reagent 1:10 in RPMI-1640 medium. Plates were subsequently incubated for 1-2 h in the dark at 37 °C. Cell viability was quantified by measuring absorbance at 570 nm with a reference wavelength of 600 nm using a Tecan Infinite® M200 PRO multimode microplate reader (Tecan Group Ltd., Switzerland).

Cell viability percentages were calculated relative to the untreated control group. Cytotoxicity interpretation was performed according to ISO 10993-5, in which a reduction in cell viability greater than 30% (cell viability below 70%) is categorized as cytotoxic. Statistical analysis was conducted using one-way analysis of variance (ANOVA) followed by Tukey's post hoc test to evaluate significant differences among treatment groups. Differences were considered statistically significant at $p < 0.05$.

Morphological observations were performed after resazurin incubation using an inverted light microscope (EVOS XL Core, Thermo Fisher Scientific, USA) to evaluate potential structural alterations, including cell shrinkage, detachment, membrane disruption, and changes in cellular adhesion. Selected samples were further examined using SEM to confirm cellular integrity and surface morphology.

3. Results and discussions

The physicochemical characteristics of the synthesized banana-template-derived nano-hydroxyapatite (nano-HA) variants, previously reported and summarized in Table 1, are presented here to provide a structural and material basis for interpreting the observed cytotoxicity behaviour. As shown in Table 1, systematic variations in crystallite size, crystallinity, particle size, surface area, pore size, and morphology are evident among NHA230B15, NHA230K15, and NHA230P15, reflecting the influence of the banana plant part used as the natural template during synthesis.

The relatively higher crystallinity observed for NHA230K15 and NHA230P15 indicates the formation of more ordered crystal structures, whereas NHA230B15 exhibited the highest specific surface area among the tested variants. These physicochemical differences are important because nano-HA biological interactions are strongly influenced by particle morphology, surface characteristics, and crystal structure [1,4]. Materials with larger surface areas generally exhibit higher surface reactivity and stronger interactions with biological environments, which may influence cellular responses during exposure [5]. However, the

Table 1
Summary of physicochemical characteristics of banana-template-derived nano-HA variants reported in previous studies.

Sample	Template source	Crystallite size (nm)	Crystallinity (%)	Particle size (nm)	Surface area (m^2/g)	Pore size (nm)	Morphology
NHA 230 B15	Banana flower	25.32	83.84	361.4	36.63	7.30	Short nanorods
NHA 230 K15	Banana pseudostem	19.57	90.27	413.8	32.14	6.92	Shortened nanorods/nanowire-derived
NHA 230 P15	Banana peel	25.45	92.02	213.3	25.85	7.42	Short nanorods

present study did not perform quantitative correlation analysis between individual physicochemical parameters and biological response. Therefore, any relationship between surface area, crystallinity, morphology, and cytotoxicity should be interpreted as an association rather than direct evidence of causality. Although dissolution behavior and ion-release kinetics were not directly evaluated in the present study, the observed variations in cytotoxic response may be associated with differences in surface-related properties rather than bulk composition, since previous XRD analysis confirmed the absence of secondary calcium phosphate phases and demonstrated comparable hydroxyapatite crystal structures among the synthesized samples [10].

Cytotoxicity evaluation of the three nano-HA variants was performed using the resazurin reduction assay on normal CV-1 fibroblast cells. This assay is based on the reduction of non-fluorescent blue resazurin into fluorescent pink resorufin by metabolically active cells, thereby serving as an indicator of mitochondrial activity and cell viability [16]. Since the resazurin assay is a well-established and widely recognized method for cytotoxicity screening, the schematic reduction mechanism is not discussed in detail in this study. Instead, the analysis focuses on the biological response of CV-1 cells following exposure to the synthesized nano-HA materials. The schematic reaction mechanism is presented in Fig. 1 to illustrate the biochemical basis of the assay. It should be noted that dedicated nanoparticle-only interference controls were not included in the present study. However, the nanoparticle-containing treatment medium was removed prior to the addition of PrestoBlue reagent, thereby reducing the direct presence of suspended particles during absorbance measurements. Nevertheless, potential nanoparticle–dye interactions or adsorption phenomena cannot be completely excluded and should be evaluated in future investigations.

The qualitative outcomes of the cytotoxicity assay are presented in Fig. 2, which shows representative well-plate images for each nano-HA variant across the tested concentration range. Most samples exhibited dominant pink coloration, indicating the preservation of cellular metabolic activity. A slight reduction in color intensity was observed for NHA230B15 at the highest tested concentration (1000 μg/mL), suggesting decreased metabolic activity relative to the other variants. Quantitative viability analysis further demonstrated that NHA230K15 and NHA230P15 maintained high cell viability throughout the tested concentration range.

According to ISO 10993-5, a reduction in cell viability greater than 30% (cell viability below 70%) is generally categorized as cytotoxic. Based on this criterion, NHA230K15 and NHA230P15 can be classified as non-cytotoxic under the tested conditions, whereas NHA230B15 demonstrated borderline cytotoxic behavior at the highest concentration tested. Nevertheless, no severe reduction in viability was observed at lower concentrations, indicating concentration-dependent biological effects. All experiments were conducted in triplicate (n = 3), and the data are presented as mean ± standard deviation. Statistical significance among treatment groups was analyzed using one-way ANOVA followed by Tukey's post hoc test, with $p < 0.05$ considered statistically significant.

Morphological evaluation was conducted to complement the quantitative viability analysis because structural cellular alterations often accompany cytotoxic responses [16]. Representative micrographs of CV-1 cells following exposure to NHA230B15 are presented in Fig. 3. Most cells retained their elongated fibroblast-like morphology, maintained adhesion to the culture substrate, and exhibited intact membrane structures. No evidence of extensive membrane rupture, severe vacuolization, or complete cell lysis was observed. However, a slight reduction in cell density became apparent at higher concentrations, which is consistent with the reduction in metabolic activity observed in the viability assay.

The morphology of CV-1 cells treated with NHA230K15 and NHA230P15 is shown in Figs. 4 and 5, respectively. In both treatments, cells remained evenly distributed and retained normal fibroblast morphology with stable adhesion and preserved membrane integrity. No apparent morphological features associated with apoptosis or severe cytotoxicity, such as cell shrinkage, detachment, or fragmentation, were

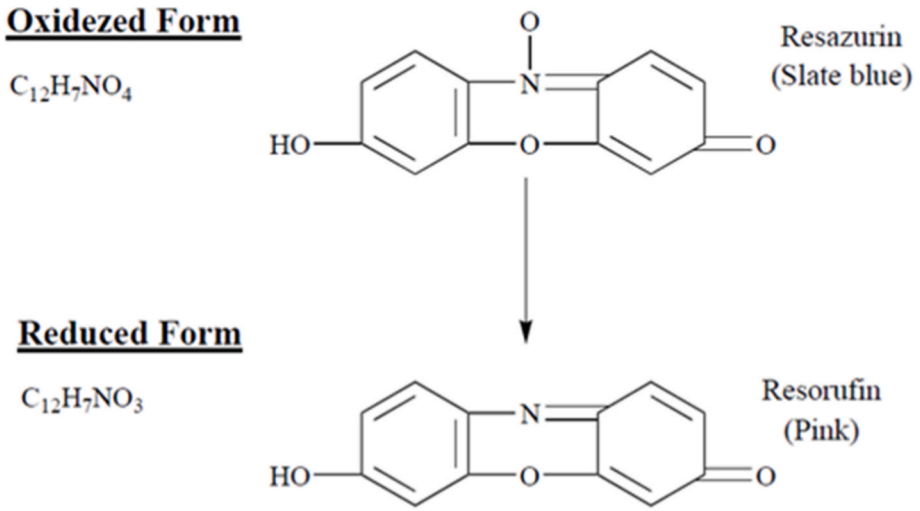

Fig. 1. Reduction and oxidation reactions of resazurin underlying the resazurin-based cell viability assay.

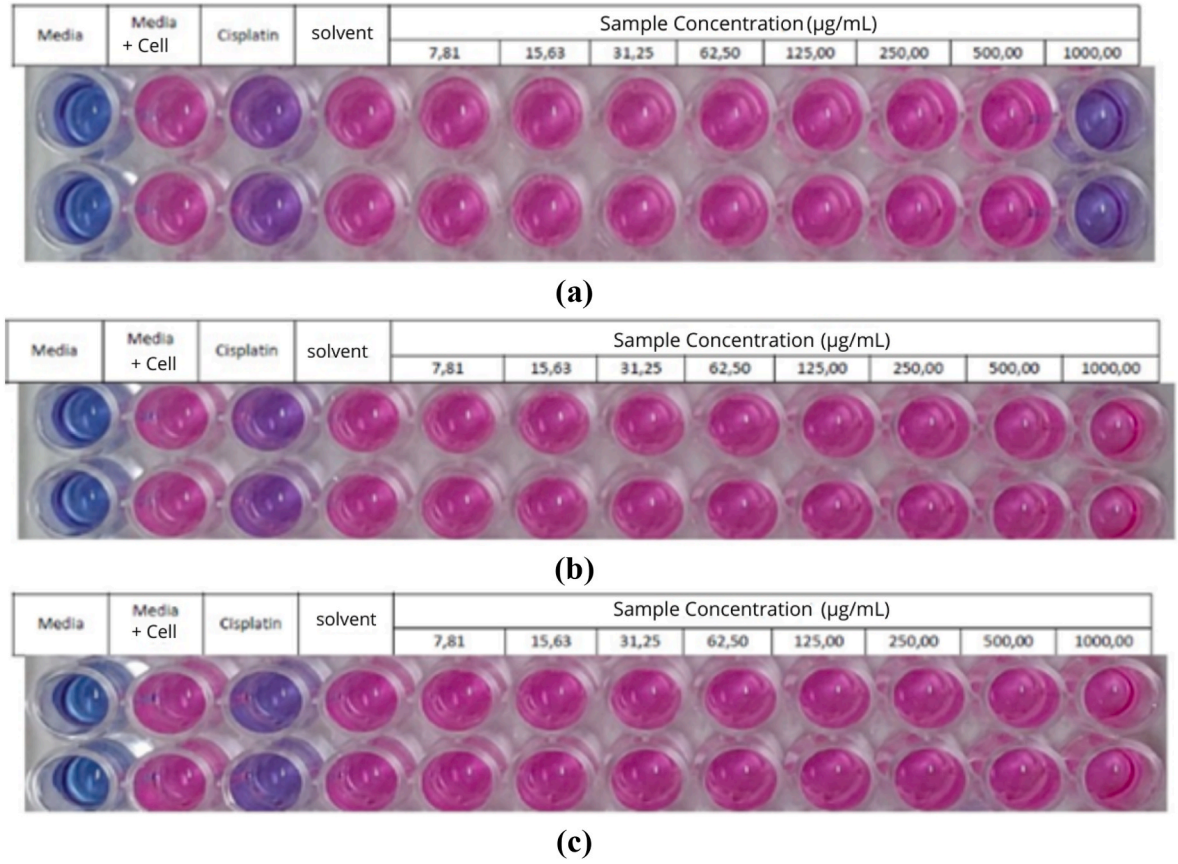

Fig. 2. Representative well-plate images showing CV-1 cell viability after exposure to (a) NHA230B15, (b) NHA230K15, and (c) NHA230P15 at various concentrations, as indicated by resazurin colour change.

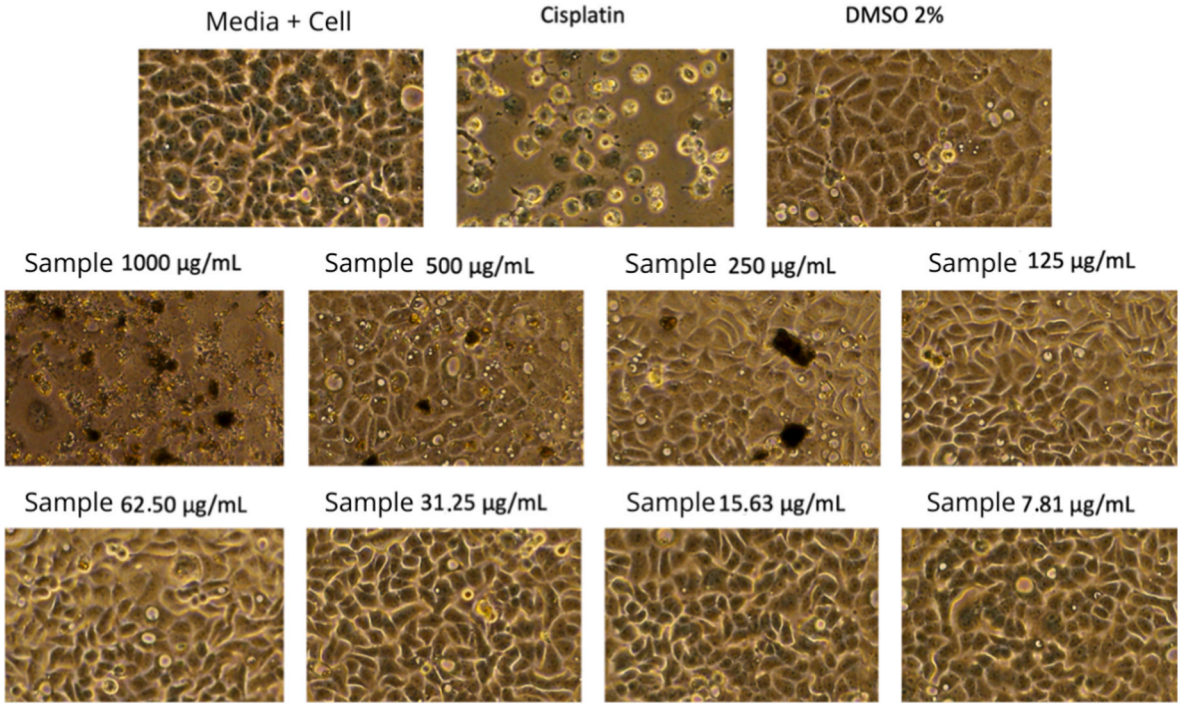

Fig. 3. Morphology of CV-1 cells after treatment with NHA230B15, showing preserved fibroblast-like structure and intact cell membranes.

detected even at the highest concentration tested. These observations are consistent with the high viability values obtained from the resazurin assay, supporting the favorable cytocompatibility profile of NHA230K15 and NHA230P15.

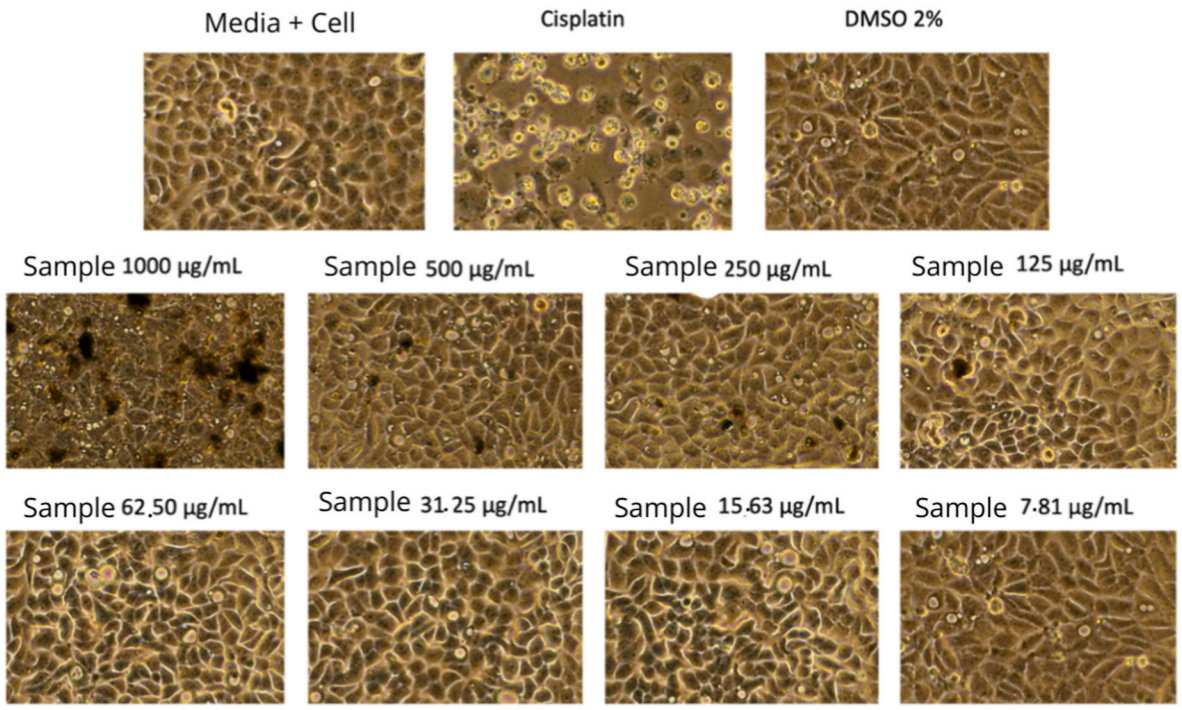

Fig. 4. CV-1 cell morphology following exposure to NHA230K15, demonstrating normal cell spreading and absence of cytotoxic morphological alterations.

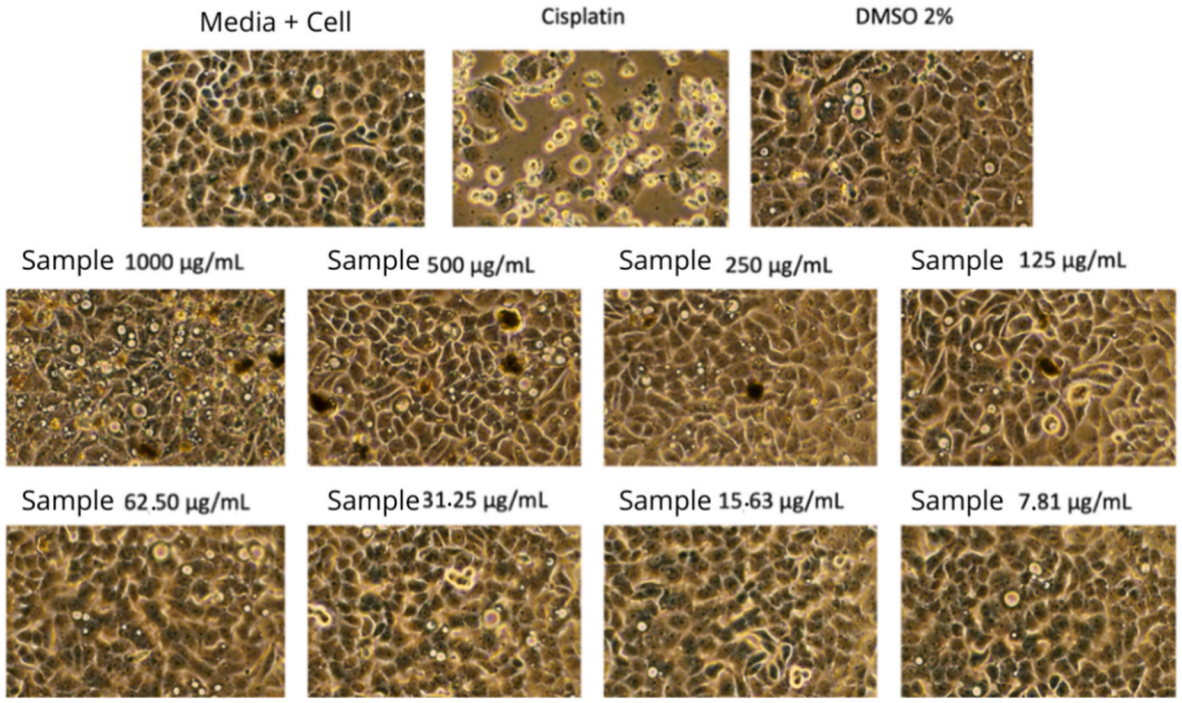

Fig. 5. CV-1 cell morphology following exposure to NHA230P15, indicating maintained cellular integrity and adhesion.

Dose–response analysis of the nano-HA variants is presented in Fig. 6. NHA230K15 and NHA230P15 did not reach IC_{50} values within the tested concentration range up to 1000 µg/mL, indicating minimal inhibitory effects on CV-1 cell proliferation. In contrast, NHA230B15 exhibited a progressive decrease in viability at elevated concentrations, approaching the cytotoxicity threshold defined by ISO 10993-5. Although the IC_{50} value was not reached within the experimental range, these findings suggest that NHA230B15 possesses relatively higher biological reactivity compared with the other variants.

The differences in cytotoxic response among the synthesized nano-HA materials may be associated with their distinct physicochemical properties, particularly surface area and morphology. Among the evaluated materials, NHA230B15 exhibited both the highest specific surface area and the lowest cell viability at elevated concentrations. However, because only three nano-HA variants were investigated, no meaningful quantitative correlation analysis could be performed. Therefore, the apparent relationship between surface area and cytotoxic response should be regarded as a qualitative observation rather than evidence of a

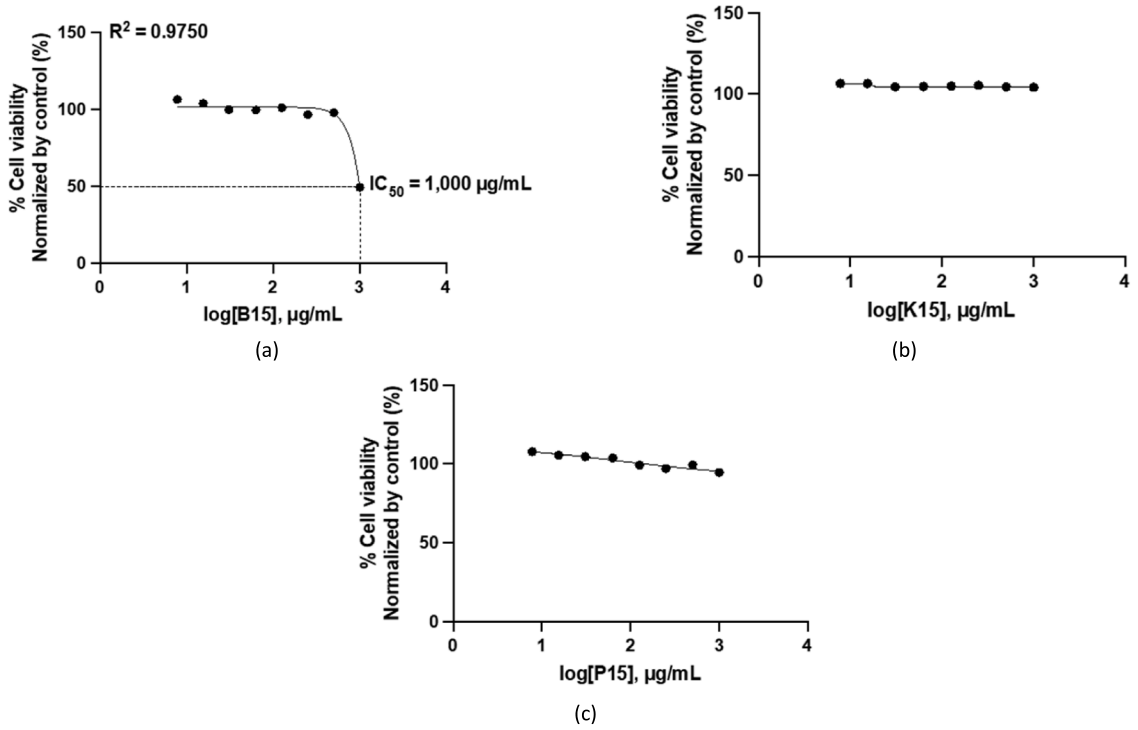

Fig. 6. Dose–response curves of CV-1 cell viability following exposure to (a) NHA230B15, (b) NHA230K15, and (c) NHA230P15, as determined by the resazurin reduction assay. Data represent mean values obtained from triplicate measurements (n = 3).

causal relationship. Previous studies have demonstrated that nano-HA materials with higher surface reactivity may induce stronger cellular responses due to increased adsorption of biomolecules and enhanced interaction with cellular membranes [5]; [1]. In addition, nanoparticle behaviour in biological media may be influenced by factors such as aggregation state, sedimentation behaviour, protein corona formation, and particle dispersion stability, which were not directly investigated in the present study. Nevertheless, the present study did not directly evaluate ion-release kinetics, dissolution behavior, reactive oxygen species generation, or intracellular nanoparticle uptake. Therefore, the proposed mechanism remains preliminary and should be interpreted cautiously. Consequently, the observed differences in cell viability should be regarded as phenomenological observations rather than mechanistic evidence.

Compared with previously reported nano-HA-based bioceramic systems, the synthesized banana-template-derived nano-HA materials demonstrated comparable cytocompatibility toward normal mammalian cells while utilizing sustainable biowaste-derived precursors and natural plant templates [17]; [9]. The porous nanorod-like morphology and moderate surface area observed in NHA230K15 and NHA230P15 may support future exploration for biomedical and biomaterial-related applications. However, additional studies involving long-term exposure, hemocompatibility, inflammatory response evaluation, drug loading capacity, and *in vivo* biocompatibility are still required before further translational application can be considered. Several limitations should also be acknowledged. The present work evaluated cytocompatibility using a single mammalian cell line (CV-1 fibroblasts) and a single metabolic viability assay following 24 h exposure. Endotoxin contamination, nanoparticle dispersion stability, protein corona formation, ion release, oxidative stress responses, and cellular uptake were not assessed. Furthermore, the biological evaluation was conducted using previously synthesized material batches and did not address batch-to-batch variability. Therefore, the current findings should be considered as a preliminary in vitro cytocompatibility assessment rather than a comprehensive biological safety evaluation.

Overall, the combination of quantitative viability analysis, dose–response evaluation, and morphological observations indicates that the synthesized banana-template-derived nano-HA materials generally exhibit favorable cytocompatibility toward normal CV-1 cells under the tested conditions. Among the evaluated samples, NHA230K15 and NHA230P15 demonstrated the most favorable biological response, whereas NHA230B15 showed increased cellular sensitivity at the highest tested concentration, likely associated with its higher surface reactivity.

4. Conclusions

The banana-template-derived nano-hydroxyapatite (nano-HA) synthesized from eggshell waste generally exhibited favorable cytocompatibility toward normal CV-1 cells under the tested conditions. NHA230K15 and NHA230P15 maintained cell viability above the ISO 10993-5 cytotoxicity threshold throughout the tested concentration range, whereas NHA230B15 showed reduced viability at the highest concentration tested, indicating relatively higher biological reactivity. Morphological observations confirmed that treated cells largely retained normal fibroblast-like morphology and membrane integrity. The differences in cytotoxic response are suggested to be associated with variations in physicochemical properties, particularly surface area and morphology. Overall, the synthesized nano-HA materials demonstrated promising characteristics for future biomedical and biomaterial-related applications, although further studies involving long-term exposure, mechanistic evaluation, and *in vivo* biocompatibility are still required.

CRediT authorship contribution statement

Atiek Rostika Noviyanti: Conceptualization, Funding acquisition, Methodology, Supervision. **Ferli Septi Irwansyah:** Writing – original draft. **Alfi Ikhlasul Amal:** Writing – original draft, Writing – review & editing. **Diana Rakhmawaty Eddy:** Supervision, Validation. **Risdiana Risdiana:** Supervision, Validation. **Yaya Rukayadi:** Supervision, Validation.

Declaration of competing interest

The authors declare that they have no known competing financial interests or personal relationships that could have appeared to influence the work reported in this paper.

Acknowledgement

This research was funded by Riset Keunggulan Keilmuan Universitas Padjadjaran (RKKU) No. 949/UN6.3.1/PT.00/2025.

Data availability

Data will be made available on request.

References

[1] C.Y. Rao, X.Y. Sun, J.M. Ouyang, Effects of physical properties of nano-sized hydroxyapatite crystals on cellular toxicity in renal epithelial cells, Mater. Sci. Eng., C 103 (2019), https://doi.org/10.1016/j.msec.2019.109807.

[2] Q.U. Ain, H. Munir, F. Jelani, F. Anjum, M. Bilal, Antibacterial potential of biomaterial derived nanoparticles for drug delivery application, Mater. Res. Express 6 (12) (2019), https://doi.org/10.1088/2053-1591/ab715d.

[3] C.C. Coelho, L. Grenho, P.S. Gomes, P.A. Quadros, M.H. Fernandes, Nano-hydroxyapatite in oral care cosmetics: characterization and cytotoxicity assessment, Sci. Rep. 9 (1) (2019), https://doi.org/10.1038/s41598-019-47491-z.

[4] O. Zakharova, A. Gusev, K. Chuprunov, A. Yudin, D. Kuznetsov, Cytotoxic effects of granulated hydroxyapatite with various particle size distribution, IOP Conf. Ser. Mater. Sci. Eng. 731 (1) (2020), https://doi.org/10.1088/1757-899X/731/1/012020.

[5] M. Awashra, P. Młynarz, The toxicity of nanoparticles and their interaction with cells: an in vitro metabolomic perspective, Nanoscale Adv. 5 (10) (2023) 2674–2723, https://doi.org/10.1039/d2na00534d.

[6] A.P. Fagundes, A.H. da Silva Júnior, D.L.P. Macuvele, H.G. Riella, N. Padoin, C. Soares, Plant-mediated synthesis of nanoscale hydroxyapatite: morphology variability and biomedical applications, in: Handbook of Green and Sustainable Nanotechnology, Springer International Publishing, 2023, pp. 537–562, https://doi.org/10.1007/978-3-031-16101-8_96.

[7] G.C.D. Putri, A.R. Noviyanti, Y.P. Budiman, S. Suryana, A.B. Ma'Amor, Microwave-assisted synthesis of eggshell-derived hydroxyapatite for antibacterial toothpaste enriched with avocado seed powder and extract, JTK (Jurnal Tadris Kimiya) 11 (1) (2026) 37–57, https://doi.org/10.15575/jtk.v11i1.55586.

[8] F.S. Irwansyah, A.I. Amal, E.P. Hadisantoso, A.R. Noviyanti, D.R. Eddy, R. Risdiana, New insight on the role of banana plant (Musa acuminata Cavendish) template in low-temperature synthesis of hydroxyapatite, Results Chem. 13 (September 2024) (2025) 101932, https://doi.org/10.1016/j.rechem.2024.101932.

[9] M. Mathina, E. Shinyjoy, L. Kavitha, D. Gopi, A preliminary study on the synthesis of biogenic derived hydroxyapatite/medicinal plant extracts composite for potential bone tissue engineering applications, Mater. Today Proc. 51 (2022) 1817–1820, https://doi.org/10.1016/j.matpr.2021.11.488.

[10] F.S. Irwansyah, A.I. Amal, E.P. Hadisantoso, A.R. Noviyanti, D.R. Eddy, R. Risdiana, S. Suryana, S.B.M. Zain, How to make and characterize hydroxyapatite from eggshell using the hydrothermal method: potential insights for drug delivery system, Indonesian J Sci Technol 8 (3) (2023) 469–486, https://doi.org/10.17509/ijost.v8i3.60825.

[11] E.J. Evans, Toxicity of hydroxyapatite in vitro: the effect of particle size, Biomaterials 12 (6) (1991) 574–576, https://doi.org/10.1016/0142-9612(91)90054-E.

[12] A.O. da Silva de Barros, E. Ricci-Junior, L.M.R. Alencar, P.B.A. Fechine, D. M. Andrade Neto, E. Bouskela, R. Santos-Oliveira, High doses of hydroxyapatite nanoparticle (nHAP) impairs microcirculation in vivo, Colloids Surf. B Biointerfaces 233 (2024), https://doi.org/10.1016/j.colsurfb.2023.113601.

[13] Y. Liu, C. Xu, T. Sun, J. Cheng, Toxicity assessment of nano-hydroxyapatite, -zeolite, and -iron tetroxide to soil fauna: the earthworm (Eisenia fetida) as a model organism, Environ. Technol. Innov. 35 (2024), https://doi.org/10.1016/j.eti.2024.103693.

[14] J. Petiti, L. Revel, C. Divieto, Standard operating procedure to optimize resazurin-based viability assays, Biosensors 14 (4) (2024) 156, https://doi.org/10.3390/bios14040156.

[15] J.S. Uzarski, M.D. DiVito, J.A. Wertheim, W.M. Miller, Essential design considerations for the resazurin reduction assay to noninvasively quantify cell expansion within perfused extracellular matrix scaffolds, Biomaterials 129 (2017) 163–175, https://doi.org/10.1016/j.biomaterials.2017.02.015.

[16] E.M. Longhin, N. El Yamani, E. Rundén-Pran, M. Dusinska, The alamar blue assay in the context of safety testing of nanomaterials, Front. Toxicol. 4 (2022) 981701, https://doi.org/10.3389/ftox.2022.981701.

[17] K. Alorku, M. Manoj, A. Yuan, A plant-mediated synthesis of nanostructured hydroxyapatite for biomedical applications: a review, RSC Adv. 10 (67) (2020) 40923–40939, https://doi.org/10.1039/D0RA08529D.